EphA4 may contribute to microvessel remodeling in the hippocampal CA1 and CA3 areas in a mouse model of temporal lobe epilepsy

LI FENG[1*], YI SHU[2*], QIAN WU[3], TIANTIAN LIU[1], HONGYU LONG[1], HUAN YANG[1], YI LI[1,4**] and BO XIAO[1**]

[1]Department of Neurology, Xiangya Hospital, Central South University, Changsha, Hunan 410008; [2]Department of Neurology, The Second Xiangya Hospital, Central South University, Changsha, Hunan 410011; [3]Department of Neurology, First Affiliated Hospital of Kunming Medical University, Kunming, Yunnan 650032, P.R. China; [4]Department of Neurology, University of Massachusetts Medical School, Worcester, MA 01604, USA

Received October 16, 2015; Accepted September 10, 2016

DOI: 10.3892/mmr.2016.6017

Abstract. Unclustered and pre-clustered ephrin-A5-Fc have identical anti-epileptic effects in the dentate gyrus of hippocampus in a mouse model of temporal lobe epilepsy (TLE), and act through alleviating ephrin receptor A4 (EphA4)-mediated neurogenesis and angiogenesis. However, the effects of ephrin-A5-Fcs on EphA4 and angiogenesis in Cornu Ammonis (CA)1 and CA3 areas remain unclear. In the present study, male C57BL/6 mice underwent pilocarpine-induced TLE. The expression of EphA4 and ephrin-A5 proteins was analyzed by immunohistochemistry, and the mean density and diameter of platelet endothelial cell adhesion molecule-1-labeled microvessels in CA1 and CA3 were calculated in the absence or presence of two types of ephrin-A5-Fc intrahippocampal infusion. Microvessels perpendicular to the pyramidal cell layer decreased; however, microvessels that traversed the layer increased, and became distorted and fragmented. The mean densities and diameters of microvessels gradually increased and remained greater than those in the control group at 56 days post-status epilepticus (SE). The upregulation of EphA4 and ephrin-A5 proteins began at 7 days and was maintained until 28 days, subsequently decreasing slightly at 56 days post-SE. Blockade of EphA4 by unclustered-ephrin-A5-Fc effected a reduction in the mean density and mean diameter of microvessels in the CA1 and CA3 areas; conversely, activation of EphA4 by clustered-ephrin-A5-Fc induced an increase in these values. Ephrin-A5 ligand binding to EphA4 receptor may contribute to angiogenesis during epileptogenesis in the hippocampal CA1 and CA3 areas.

Correspondence to: Dr Bo Xiao, Department of Neurology, Xiangya Hospital, Central South University, 87 Xiangya Road, Changsha, Hunan 410008, P.R. China
E-mail: mdboxiao@163.com

Dr Yi Li, Department of Neurology, University of Massachusetts Medical School, 55 Lake Avenue North, Worcester, MA 01604, USA
E-mail: yi.li@umassmemorial.org

*Contributed equally; **Joint senior authorship

Key words: ephrin receptor A4, platelet endothelial cell adhesion molecule-1, angiogenesis, hippocampus, temporal lobe epilepsy, pilocarpine

Introduction

Temporal lobe epilepsy (TLE) is the most prevalent type of partial complex seizures in the clinical setting; seizures in 20-30% of TLE patients are poorly controlled by anti-epileptic drugs (1). An alternative method to examine the potential mechanisms underlying epileptogenesis is through the use of animal models. The pilocarpine model of TLE in mice was first described in 1983 (2), and is an animal model that mimics the pathology of human TLE. Initially, the mice undergo an acute period that begins with pilocarpine-induced status epilepticus (SE), which is followed by a latent period lasting no more than 14 days in which mice demonstrate normal behavior and electroencephalograph activity, although the pathophysiological processes associated with epileptogenesis may occur. Subsequently, the mice exhibit spontaneous recurrent seizures (SRSs), described as the key characteristic of the chronic period (3). Following SE, there are a series of pathophysiological processes in the hippocampal Cornu Ammonis (CA) areas that reorganize the epileptogentic neurological networks. Neurodegeneration (4,5), neurogenesis (6), mossy fiber sprouting (MFS) (3,7) and dendrite spine plasticity (8,9) are the most extensively described pathological changes. These neurobiological phenomena require excessive oxygen and glucose. It has been observed that the hippocampal cerebral blood volume of mice remained elevated for two weeks following pilocarpine-induced SE using magnetic resonance imaging, and that the hippocampal vessel morphology of the rats altered using immunochemistry (10); however, the cerebral blood flow was not altered (10). The molecular mechanisms underlying the angiogenesis of epilepsy remain to be fully elucidated.

The erythropoietin-producing hepatocellular family of receptor tyrosine kinases (Eph receptors) is one of the largest

families of receptor tyrosine kinases. They comprise a glycosylated extracellular domain including an immunoglobulin-like ligand-binding site, a cysteine-rich region and two fibronectin (FN) type III repeats. This is connected via a transmembrane domain to the intracellular domain, consisting of a juxtamembrane region, a protein tyrosine kinase region, a sterile alpha motif, and a postsynaptic density 95-discs large-zonula occludentes-1 binding motif (11). The ephrins, as the ligands of Eph receptors, are divided into two subfamilies: Ephrin-As associate with the cell membrane via a glycosylphosphatidylinositol anchor, and ephrin-Bs span the cell membrane and contain a cytoplasmic domain. EphA receptors preferentially bind all ephrin-As and EphB receptors bind all ephrin-Bs; however, EphA4 binds ephrin-As and -Bs. To date, three interaction sites have been identified between EphA4 and ephrin-As: The high affinity interface of G -H_L loop in ephrin-As and the hydrophobic pocket in EphA4, the low affinity interface of solvent-excluded regions at the ephrin-docking site along the upper convex surface of the receptor, and the clustering interface between the ligand binding domain and the second FN located in the adjacent cysteine-rich region of the receptor (12,13). EphA4 has a series of crucial functions in the brain during embryonic development and postnatal plasticity, and is expressed in the cortex, hippocampus, corpus striatum and spinal cord (14,15). As a mediator of axon repulsion, EphA4 contributes to the localization of the position of growth cone and nerve projection (16,17). During neurogenesis, EphA4 is considered to regulate neural stem/progenitor cell proliferation, differentiation and migration (18). Furthermore, previous studies have suggested that EphA4 may regulate angiogenesis in the neural system (19,20). Following deletion of ephrin-A5 in mice, EphA4 was blocked and hippocampal vessels were narrowed (19). In addition, EphA4 was revealed to regulate vascular smooth muscle contractility (20). As vessel remodeling is induced by EphA4, this receptor may be a key mediator in angiogenesis during epileptogenesis. Our previous study demonstrated that in the hippocampal dentate gyrus the microvessel density decreased following EphA4 reduction (21). Ephrin-A-Fc is a genetically-engineered immunoadhesin that targets EphA receptors; it contains the natural receptor binding domain of endogenous ephrin-A to interact with EphA receptors and it is capable of eliciting dimerization and thus phosphorylation of its receptor (22). There are two types of ephrin-A-Fc: The unclustered form and the pre-clustered form. The former is typically an antagonist that blocks EphA expression and the latter is an agonist that activates EphA expression (23-25). However, our previous study revealed that the unclustered and pre-clustered ephrin-A5-Fc had the same inhibition effect on EphA4 (21).

Therefore, the present study investigated the expression of the angiogenesis-associated protein EphA4 and its ligand ephrin-A5, and the plasticity of platelet endothelial cell adhesion molecule-1 (PECAM-1)-labeled microvessels in the hippocampal CA1 and CA3 areas in a mouse model of TLE induced by pilocarpine. The results of the present study demonstrated the effects of two opposite types of ephrin-A5-Fc on EphA4 and microvessel remodeling.

Materials and methods

Animal model. A total of 91 male C57BL/6 mice (weight, 18-21 g; age, 5-6 weeks; specific pathogen-free) were purchased from the Experimental Animal Center of Central South University (Changsha, China). Mice were housed at 5-6 per cage, at a temperature of 23±1˚C under a 12-h light/dark cycle, and had *ad libitum* access to food and water. The animals were maintained in accordance with the National Institutes of Health Guide for the Care and Use of Laboratory Animals, and the present study was approved by the Animal Ethics Committee of Central South University. The animals were randomly divided into experimental and control groups and treated with pilocarpine as previously described (26). All animals received an intraperitoneal injection of 1 mg/kg scopolamine hydrobromide (Shanghai Harvest Pharmaceutical Co., Ltd., Shanghai, China) 30 min prior to pilocarpine injection. Subsequently, a total of 67 mice received an intraperitoneal injection of 320-340 mg/kg pilocarpine (Sigma-Aldrich; Merck Millipore, Darmstadt, Germany) diluted in sterile saline, which induced SE followed by hippocampal damage and the development of SRSs. In the present study, 36 mice recovered from SE and 31 mice died. Mice in the control group (n=24) received an injection of the same volume of sterile saline instead of pilocarpine. All mice received an intraperitoneal injection of 7.5 mg/kg diazepam (Abbott Laboratories, Chicago, IL, USA) 2 h following the onset of SE to stop or limit behavioral seizures. Additional diazepam was administered if seizures were not attenuated sufficiently or recurred within 1 h following the first diazepam injection. The present study used the minimum number of animals required.

The first SRS appeared in mice 3-10 days following pilocarpine injection. A total of 24 experimental mice and the same number of control mice were sacrificed at 7, 14, 28 and 56 days post-SE (n=6 per group), which meant that none of them was removed from analysis during the study. Mice were anesthetized with an intraperitoneal injection of 10% chloral hydrate (0.05-0.1 ml/10 g; Department of Pharmacy, The Third Xiangya Hospital, Changsha, China), and perfused through the left ventricle with 0.9% sterile saline at 4˚C, followed by 4% paraformaldehyde. Following perfusion, the animals were maintained at 4˚C for 30 min, decapitated and the brains removed from the skull and postfixed in 4% paraformaldehyde for 12-16 h at 4˚C. Subsequent to thorough rinsing in phosphate buffer, the brains were cryoprotected in a 30% sucrose solution for 48-72 h and sectioned at 30 μm on a cryostat. Sections were preserved in a cryoprotectant solution (a mixture of glycerine, ethanediol and 0.1 M phosphate buffer, at a volume ratio of 5:6:9) at -20˚C until processing.

Immunohistochemistry. Free-floating sections were processed for immunohistochemistry. Following washing in phosphate-buffered saline (PBS; 0.1 M, pH 7.5) twice, sections were immersed in 1% H_2O_2 for 30 min, and antigen-retrieval was performed in sodium citrate solution (pH 6.0) using heat in a microwave for 20 min. Sections were incubated in 10% normal goat or rabbit serum in PBS containing 200 μl/ml avidin (Avidin/Biotin Blocking kit; catalog no. SP-2001; Vector Laboratories, Inc., Burlingame, CA, USA) for 2 h. The sections were rinsed gently in PBS twice between steps. The primary antibodies goat anti-ephrin-A5 (1:50; catalog no. AF3743; R&D Systems, Inc., Minneapolis, MN, USA), rabbit anti-EphA4 (1:100; catalog no. ab5396; Abcam, Cambridge, MA, USA) or rat anti-PECAM-1 (1:100; catalog no. 550274; BD Biosciences, Franklin Lakes, NJ, USA) were diluted in PBS

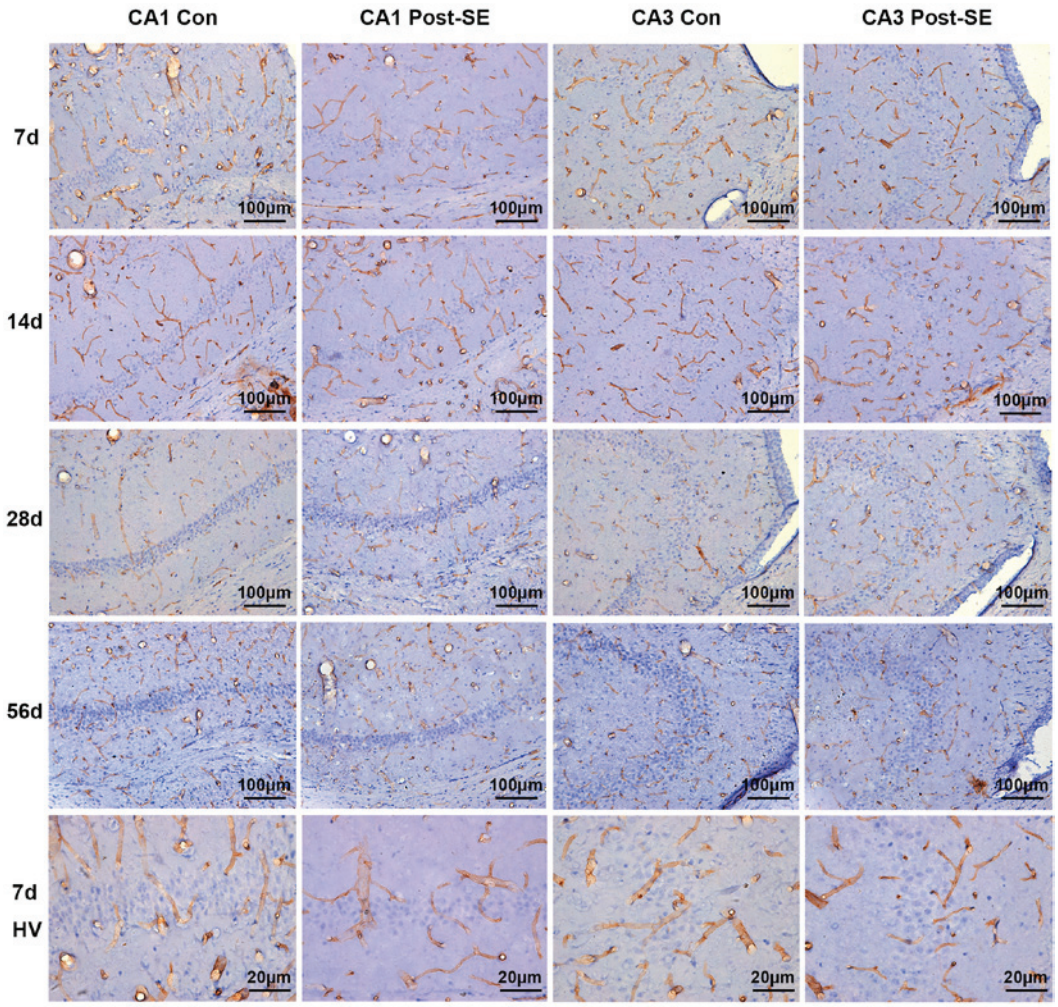

Figure 1. Immunohistochemistical staining of PECAM-1-labeled microvessels in the hippocampal CA1 and CA3 areas. Samples were harvested at 7, 14, 28 and 56 days post-SE and stained for PECAM-1. PECAM-1 staining appears brown; hematoxylin counterstaining of neural cells appears blue. Scale bars represent 100 μm in the first four rows and 20 μm in the last row. PECAM-1, platelet endothelial cell adhesion molecule 1; CA, Cornu Ammonis; SE, status epilepticus; HV, high view; Con, control group; d, day.

with 10% normal serum and 200 μl/ml biotin (Avidin/Biotin Blocking kit) and the sections were subsequently incubated in the mixed solution for 48 h at room temperature. Following rinsing in PBS, sections were incubated in PBS containing the corresponding peroxidase-labeled anti-goat, anti-rabbit, and anti-rat secondary antibody (all 1:200; catalog nos. 14-13-06, 074-1506 and 14-16-06; KPL, Inc., Gaithersburg, MD, USA) at room temperature for 1 h. VECTASTAIN® ABC kit (catalog no. PK-4000; Vector Laboratories, Inc.) and 3,3'-diaminobenzidine solution (Beijing Zhongshan Golden Bridge Biotechnology Co., Ltd., Beijing, China) were used for visualization of the immunolabeled products. Sections were counterstained with hematoxylin following PECAM-1 staining. Subsequent to dehydration, clearing and coverslipping, the sections were imaged with a DM5000 B light microscope (Leica Microsystems GmbH, Wetzlar, Germany). Imaging-Pro Plus software version 6.0 (IPP 6.0; Media Cybernetics, Inc., Rockville, MD, USA) was used to calculate the optical density (OD) values of immunolabeling products. Three unilateral hippocampal CA1 and CA3 regions were analyzed for each mouse and the mean OD value was obtained.

The microvessel densities (MVDs) and diameters of microvessels in the CA1 and CA3 hippocampal areas were calculated on a 2D plane of the images using IPP 6.0. The MVD was defined as the numbers of microvessels/total area. The mean diameter (μm) was defined as the sum of diameters/number of diameter-calculated microvessels. A total of three hippocampal sections from each mouse were examined. All longitudinal vessels were measured. Each branch of the vessel was considered as an individual vessel. Vessels crossing the section were not calculated to avoid any false positive due to edge effects around potential holes in the tissue. All measurements were conducted by researchers blinded to the animal treatment groups.

Intrahippocampal infusion. A total of 3 days following pilocarpine treatment, 12 of the treated mice were divided into 4 groups (n=3 per group), which subsequently received continuous intrahippocampal infusion in the left side using ALZET® 1007D micro-osmotic pumps (DURECT Corporation, Cupertino, CA, USA) with standard ALZET brain infusion kits. The contents of the pumps were as follows:

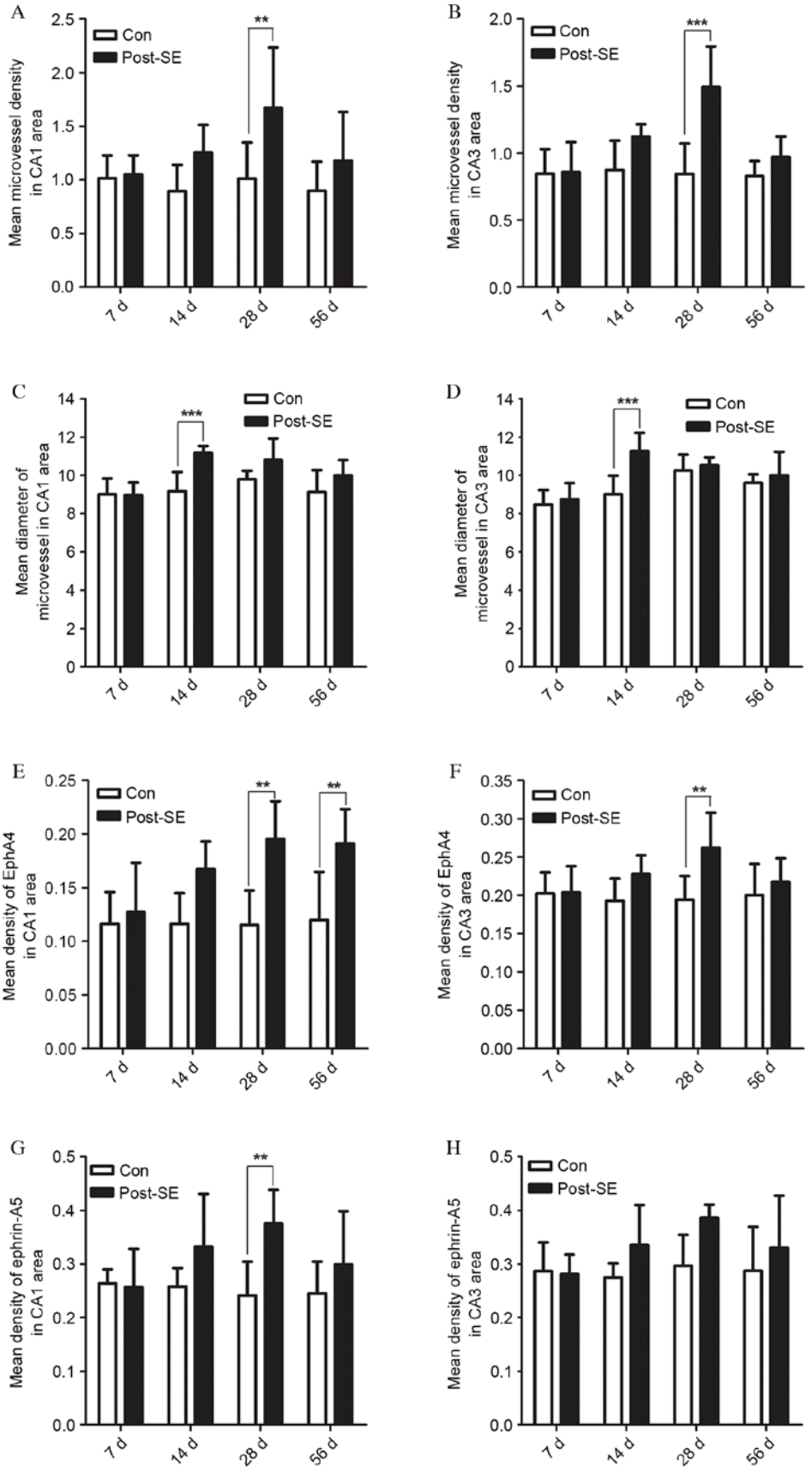

Figure 2. Mean density and diameters of microvessels, and expression of EphA4 and ephrin-A5. The mean density of PECAM-1-labeled microvessels was calculated in the (A) CA1 and (B) CA3 areas. The mean diameter of PECAM-1-labeled microvessels was calculated in the (C) CA1 and (D) CA3 areas. EphA4 expression was assessed in the (E) CA1 and (F) CA3 areas. Ephrin-A5 expression was assessed in the (G) CA1 and (H) CA3 areas. The mean density and diameter of microvessels, and the expression of EphA4 and ephrin-A5, all increased post-SE compared with control groups. Data are expressed as the mean ± standard deviation (n=6). **P<0.01; ***P<0.001. EphA4, ephrin receptor A4; PECAM-1, platelet endothelial cell adhesion molecule-1; CA, Cornu Ammonis; SE, status epilepticus; Con, control group; d, day.

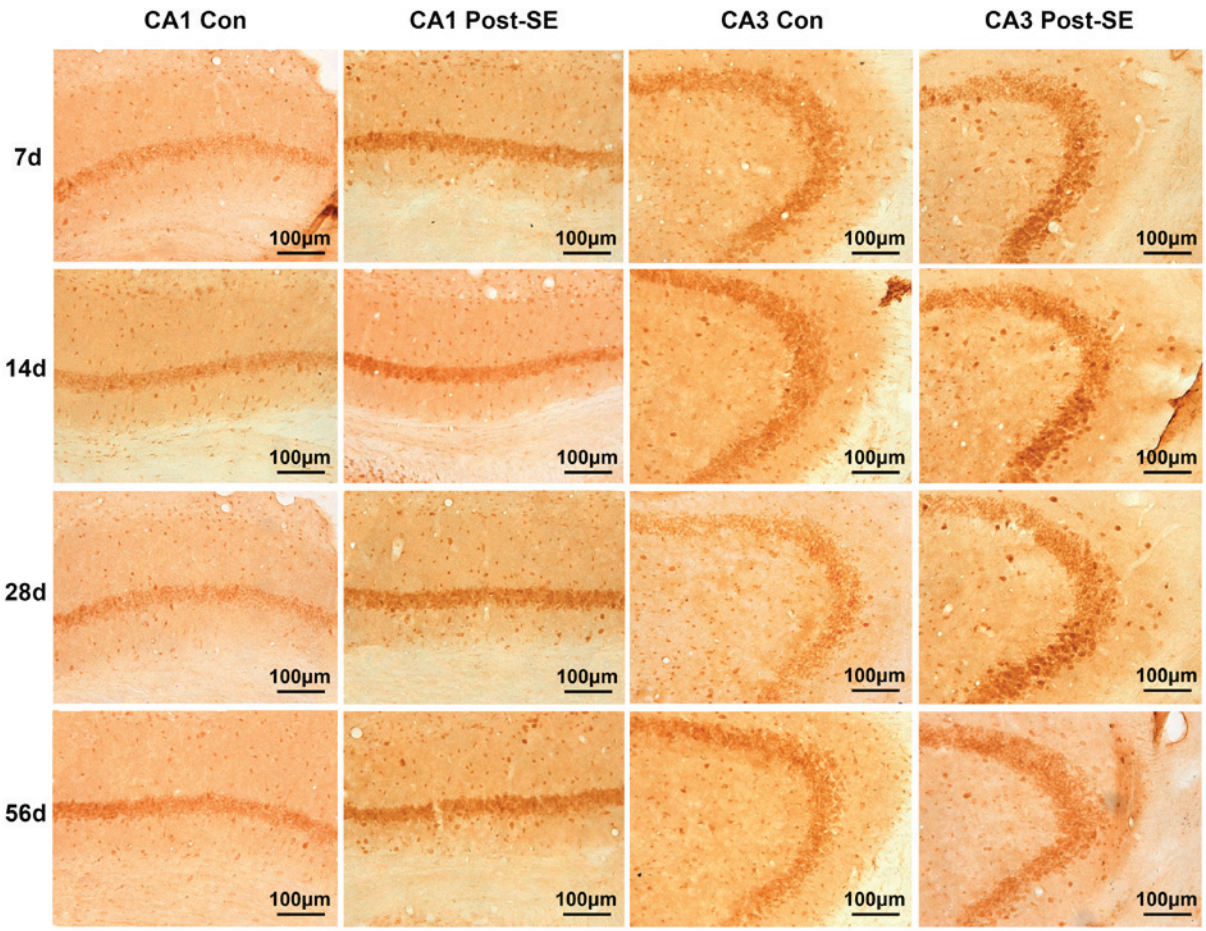

Figure 3. Immunohistochemistical staining of EphA4 in the hippocampal CA1 and CA3 areas. Samples were harvested at 7, 14, 28 and 56 days post-SE and stained for EphA4. EphA4 staining appears brown. Scale bars represent 100 μm. EphA4, ephrin receptor A4; CA, Cornu Ammonis; SE, status epilepticus; Con, control group; d, day.

Artificial cerebrospinal fluid (ACSF) negative control group, in which the pump contained only ACSF (pH 7.42) containing 124 mM NaCl, 3 mM KCl, 2.4 mM $CaCl_2$, 2.4 mM $MgSO_4$, 1.25 mM KH_2PO_4, 26 mM $NaHCO_3$ and 10 mM D-glucose; IgG_{2A} control group, using a biologically non-active IgG in ACSF, in which the pump contained 50 μg/ml mouse IgG_{2A} isotype control (catalog no. MAB003; R&D Systems, Inc.) in ACSF; non-clustered (NC)-ephrin-A5-Fc group, in which the pump contained 50 μg/ml unclustered ephrin-A5-Fc (catalog no. 7396-EA-050; R&D Systems, Inc.) in ACSF; and clustered (C)-ephrin-A5-Fc group, in which the pump contained pre-clustered ephrin-A5-Fc (50 μg/ml ephrin-A5-Fc and 500 μg/ml goat anti-mouse IgG-Fc, catalog no. G-202-C; R&D Systems, Inc.) in ACSF.

The pumps were filled, connected to a cannula and immersed in PBS at 37˚C overnight. Mice were anesthetized with an intraperitoneal injection of 10% chloral hydrate 4 days following pilocarpine treatment. Using a stereotaxic apparatus a cannula was placed into the left hippocampus of the mice at the following position: Anteriorposterior = -1.5 mm, medial lateral = -1.8 mm from bregma and dorsal ventral = 1.8 mm from flat skull surface. The cannula was cemented onto the skull with dental acrylic, the pump was placed subcutaneously in the back of mouse, and the incision was sutured. The osmotic pumps were taken out under the anesthesia 7 days later. For the following 2 weeks the SRSs were observed and recorded using video monitoring. All mice survived, and no apparent behavioral discomfort was observed. At day 28 following pilocarpine injection, the mice were sacrificed for immunohistochemistry.

Statistical analysis. Data are expressed as the mean ± standard deviation and were analyzed in GraphPad Prism software version 5.01 (GraphPad Software, Inc., La Jolla, CA, USA). Dynamic temporal expression patterns in EphA4 and ephrin-A5 proteins and vascular parameters were performed with two-way analyses of variance (ANOVA) followed by the Bonferroni correction. Statistical analyses of other data were performed with one-way ANOVA followed by Tukey's post-hoc test. $P<0.05$ was considered to indicate a statistically significant difference.

Results

Density and diameter of microvessels post-SE. In the control group, PECAM-1-labeled microvessels appeared to primarily orient perpendicular to the pyramidal cell layer (PCL) in the CA1 and CA3 areas. They mostly originated in the fissure around the cell layer. In addition, there were certain microvessels aligned in parallel to the PCL in the two

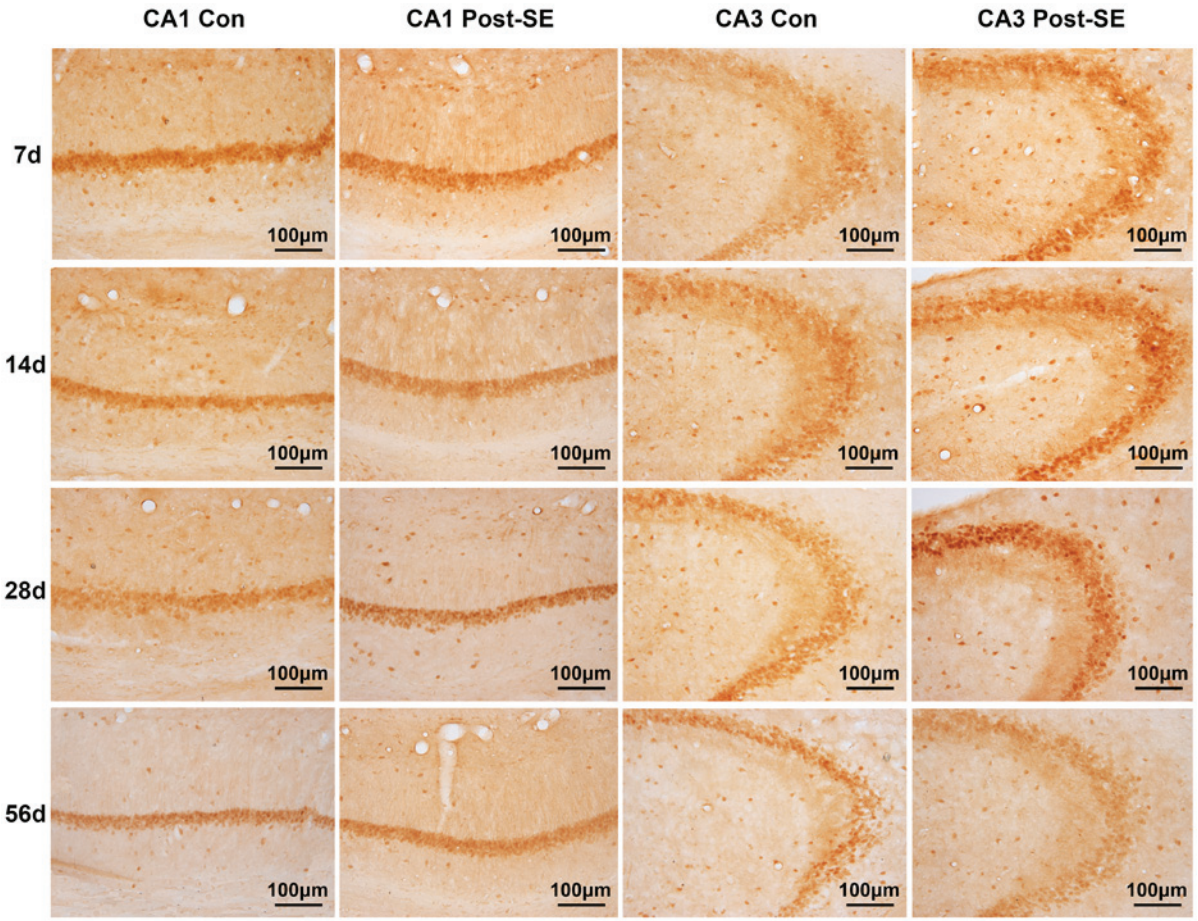

Figure 4. Immunohistochemistical staining of ephrin-A5 in the hippocampal CA1 and CA3 areas. Samples were harvested at 7, 14, 28 and 56 days post-SE and stained for ephrin-A5. Ephrin-A5 staining appears brown. Scale bars represent 100 μm. CA, Cornu Ammonis; SE, status epilepticus; Con, control group; d, day.

areas. No differences were observed in the distribution of PECAM-1-labeled microvessels in the control groups at different time points (Fig. 1). The diameter of the microvessels in CA1 was 9.272±0.3526 μm and in CA3 was 9.330±0.7638 μm. At day 7 post-SE, the mean diameter of microvessels remained comparatively stable. Although certain vessels still emanated from the fissure perpendicular to the PCL, certain others began to traverse the cell layer and became entangled to form a disorganized vascular plexus around the layer (Fig. 1). The microvessels enlarged and appeared more distorted compared with the control at 14 days post-SE (Fig. 1). At 28 days post-SE, the enlarged microvessels were more fibrous and fragmented. The individual vessels perpendicular to the PCL almost disappeared and instead intertwined vessels, which penetrated into the cell layer or around, were observed (Fig. 1). At 56 days post-SE, the mean diameter and density of microvessels recovered to a certain extent. Traversed and the vertical microvessels were observed.

The MVD in the CA1 and CA3 areas gradually increased from 7 days post-SE and peaked at 28 days post-SE ($P<0.01$). At 56 days post-SE the MVD was 70.46 and 64.98% in the CA1 and CA3 areas, respectively, of the levels at 28 days post-SE, but remained greater compared with the control (Fig. 2A and B). In the CA1 area, the mean diameters at 7, 14, 28 and 56 days post-SE were 8.9571±0.6714, 11.1698±0.3598, 10.7992±1.1180 and 9.9919±0.8019 μm, respectively; this was 0.9947-, 1.2189-, 1.1030- and 1.0946-fold, respectively, of the corresponding control groups (Fig. 2C). In the CA3 area, the mean diameters at 7, 14, 28 and 56 days post-SE were 8.743±0.8527, 11.27±0.9481, 10.53±0.4096 and 9.996±1.231 μm; this was 1.0324-, 1.2515-, 1.0283- and 1.0408-fold, respectively, of the corresponding control groups (Fig. 2D).

Expression of EphA4 and ephrin-A5 post SE. To investigate the mechanism underlying the involvement of EphA4 in hippocampal angiogenesis during epileptogenesis, the expression and distribution of EphA4 and ephrin-A5 in the CA1 and CA3 areas in the epileptic mice hippocampus were initially determined. The protein expression of EphA4 increased steadily from 7 to 28 days post-SE and subsequently plateaued (Fig. 2E and F). In the CA1 area the differences between the post-SE and control groups were significant at 28 and 56 days ($P<0.01$) and in the CA3 area significance was observed at 28 days ($P<0.01$). Similarly, the expression of ephrin-A5 protein in CA1 area increased gradually from 7 to 28 days post-SE compared with the corresponding control groups with a slight decrease at 56 compared with 28 days post-SE, although expression remained greater compared

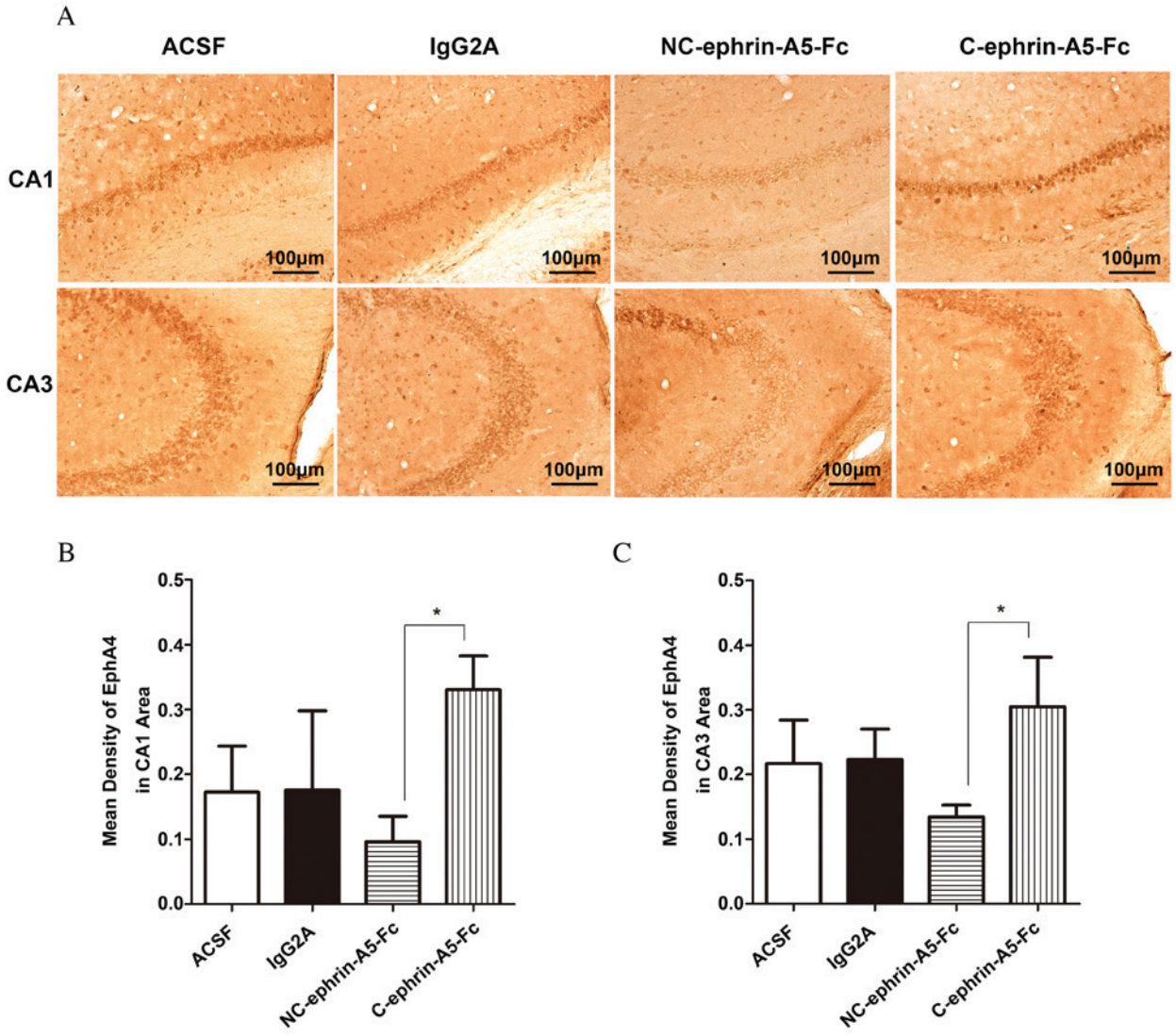

Figure 5. Expression of EphA4 in the hippocampal CA1 and CA3 areas following ephrin-A5-Fc intrahippocampal infusions. Mice received intrahippocampal infusions of ACSF, IgG_{2A} isotype control, NC-ephrin-A5-Fc or C-ephrin-A5-Fc via micro-osmotic pump for 7 days, beginning 4 days following pilocarpine treatment. (A) Immunohistochemistical staining of EphA4, which appears brown. The expression of EphA4 was analyzed in the (B) CA1 and (C) CA3 areas, and was reduced by NC-ephrin-A5-Fc and increased by C-ephrin-A5-Fc. Data are expressed as the mean ± standard deviation (n=3). *P<0.05. Scale bars represent 100 μm. EphA4, ephrin receptor A4; CA, Cornu Ammonis; ACSF, artificial cerebrospinal fluid; NC, non-clustered; C, clustered.

with the control (Fig. 2G). In the CA3 area there was no difference in the 7 day post-SE group and the control group; however, ephrin-A5 increased from 14 to 28 days post-SE compared with the control and declined slightly at 56 days post-SE (Fig. 2H). There was a significant difference between the post-SE and control groups in the CA1 area at 28 days (t=3.364; P<0.01); however, no significant differences were observed in the CA3 area. EphA4 and ephrin-A5 staining are presented in Figs. 3 and 4, respectively.

Effect of ephrin-A5-Fc infusion on EphA4 expression. To further address whether EphA4 mediates angiogenesis in the epileptic hippocampus, ephrin-A5-Fc immunoadhesin was stereotactically injected into the hippocampus. The expression of EphA4 decreased in the NC-ephrin-A5-Fc group and increased in C-ephrin-A5-Fc group compared with the ACSF and IgG_{2A} control groups in CA1 and CA3 areas; however, no statistically significant differences were observed using Tukey's post-hoc test (Fig. 5). Compared with C-ephrin-A5-Fc group, EphA4 expression was significantly reduced in the NC-ephrin-A5-Fc group in the CA1 and CA3 areas (P<0.05). No statistically significant differences were observed between the control groups.

Effect of ephrin-A5-Fc infusion on density and diameter of microvessels. The MVDs and mean diameters of microvessels in the CA1 and CA3 areas of the slices were calculated following PECAM-1 staining (Fig. 6A). Compared with the ACSF and IgG_{2A} control groups, the MVD of microvessels in the CA1 area decreased in the NC-ephrin-A5-Fc group (P<0.05) and increased in the C-ephrin-A5-Fc group (P>0.05; Fig. 6B). MVD in the CA3 area revealed a similar pattern, but with no significant differences compared with the ACSF and IgG_{2A} groups (Fig. 6C). However, the MVD in the NC-ephrin-A5-Fc group was 34.71% of that in the C-ephrin-A5-Fc group in the CA1 area (P<0.01), and

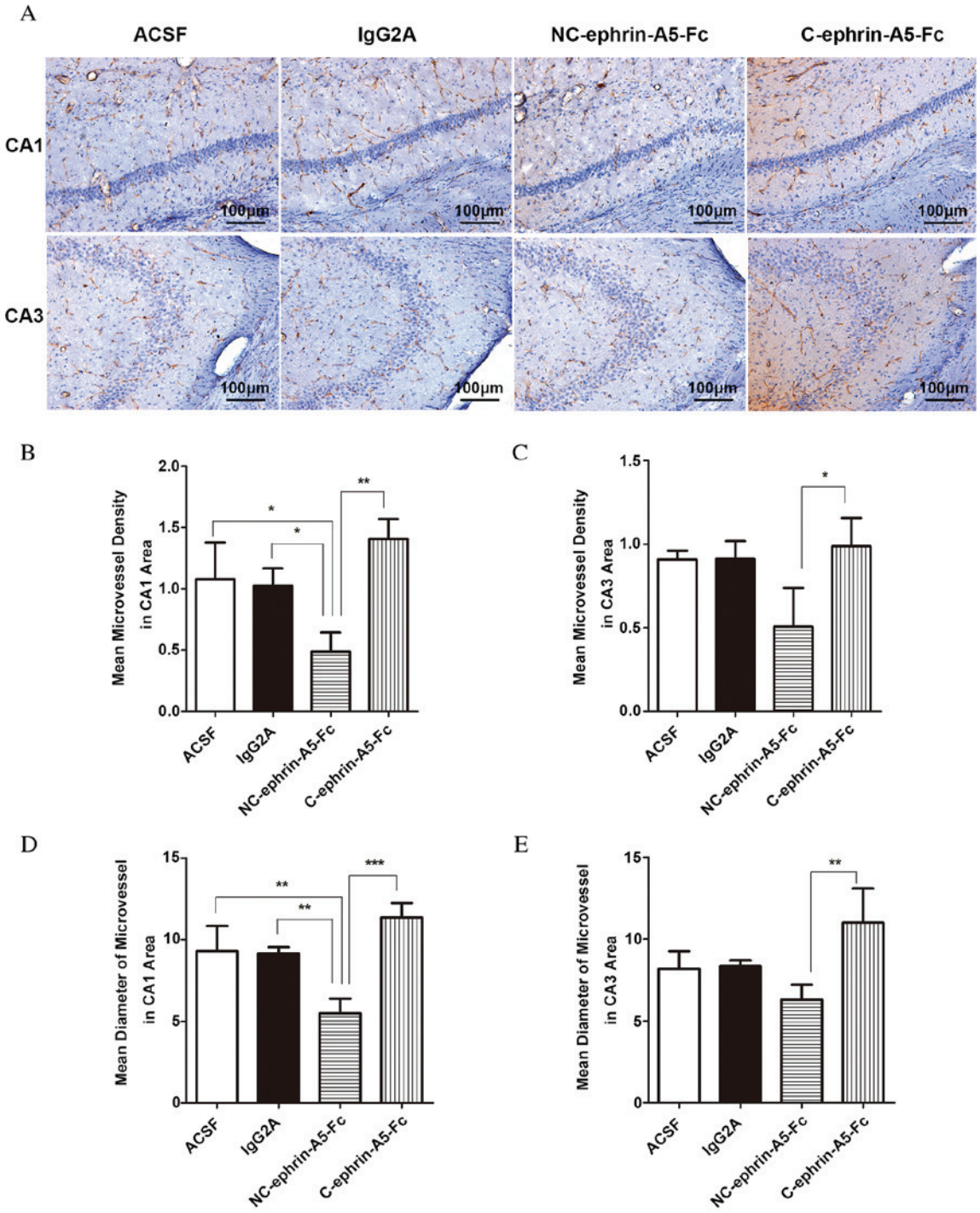

Figure 6. Mean density and mean diameter of PECAM-1-labeled microvessels in the hippocampal CA1 and CA3 areas following ephrin-A5-Fc intrahippocampal infusions. Mice received intrahippocampal infusions of ACSF, IgG_{2A} isotype control, NC-ephrin-A5-Fc or C-ephrin-A5-Fc via micro-osmotic pump for 7 days, beginning 4 days following pilocarpine treatment. (A) Immunohistochemistical staining of PECAM-1. PECAM-1 staining appears brown; hematoxylin counterstaining of neural cells appears blue. The mean density of PECAM-1-labeled microvessels was calculated in the (B) CA1 and (C) CA3 areas. The mean diameter of PECAM-1-labeled microvessels was calculated in the (D) CA1 and (E) CA3 areas. The mean density and diameter of microvessels were reduced by NC-ephrin-A5-Fc and increased by C-ephrin-A5-Fc. Data are expressed as the mean ± standard deviation (n=3). *P<0.05; **P<0.01; ***P<0.001. Scale bars represent 100 μm. PECAM, platelet endothelial cell adhesion molecule; CA, Cornu Ammonis; ACSF, artificial cerebrospinal fluid; NC, non-clustered; C, clustered.

51.29% in the CA3 area (P<0.05). The microvessels in the NC-ephrin-A5-Fc group were narrower compared with the ACSF and IgG_{2A} groups (P<0.01; Fig. 6D). The mean diameter in the CA3 area revealed a similar pattern, but without significant differences compared with the ACSF and IgG_{2A} groups (Fig. 6E). The mean diameter in the NC-ephrin-A5-Fc group was 48.35% of that in the C-ephrin-A5-Fc group in the CA1 area (P<0.001), and 57.21% in the CA3 area (P<0.01). No statistically significant differences were observed between the control groups.

Discussion

The present study demonstrated that microvessels labeled with PECAM-1 in adult hippocampal CA1 and CA3 areas of mice were influenced temporally by epileptogenesis. Expression of the receptor EphA4, and its ligand ephrin-A5, increased in the CA1 and CA3 areas during epileptogenesis. Upon removal of its ligand using NC-ephrin-A5-Fc, EphA4 expression was downregulated and the microvessels density and diameter decreased; however, when ephrin-A5 was initiated with C-ephrin-A5-Fc, EphA4 expression increased and the microvessels demonstrated greater disorganization.

Recombinant soluble ligand-type immunoadhesins appear to act as antagonists and downregulate EphA4 receptor expression; these may be converted to an agonistic reagent via artificial clustering. In the present study, EphA4 affected the morphology of microvessels and was inhibited by NC-ephrin-A5-Fc; C-ephrin-A5-Fc had the opposite function. Previous studies have revealed that EphA4 may be blocked by unclustered ephrin-A5-Fc to promote axonal regeneration (23); however, clustered ephrin-A5-Fc facilitated EphA4 expression and activated astrocyte proliferation (27). These studies have primarily been performed *in vivo*. Further studies are required to investigate the distinct underlying mechanisms of EphA4 and ephrin-A5 interaction in the mediation of endothelial proliferation, migration and vessel remodeling *in vitro*.

In addition to its role in angiogenesis, EphA4 contributes to other hippocampal remodeling processes that are relevant to epileptogenesis. The traditional neurogenesis pool in the subgranular zone of dentate gyrus is triggered by SE and SRSs (26). EphA4 is associated with apoptosis of neural cells in the hippocampus, and maintains neural stem/progenitor cells (NSC/NPC) in an undifferentiated state; its downregulation may therefore damage NPC proliferation and accelerate premature differentiation (18,28). Recently, it has been discovered that neurogenesis may exist in the CA fields serving as a vascular stem cell niche post-SE (6). Although in the present study EphA4 dynamic expression was associated with angiogenesis affected by seizures in the CA1 and CA3 areas, whether EphA4 is involved in this novel niche requires further investigation. Additionally, EphA4 is critical for rewiring dendritic synaptic circuits (29) and regulating repulsive axon guidance (30). Electron microscopic immunocytochemistry analysis has revealed that EphA4 is enriched in the myelinated/unmyelinated axons, axon terminals and dendritic spines of the CA1 and CA3 fields (31). Activated EphA4 induces spine retraction, whereas blocked EphA4 disrupts synaptogenesis in the hippocampal pyramidal cells (29). Furthermore, EphA4 may be involved in epileptic network establishment. Glutamate transporter subtype-1 (GLT-1) is essential for maintaining the balance between excitatory and suppressive networks, and the long-term potential (LTP) is critical for memory and other cognitive impairments in TLE. EphA4 affects GLT-1 levels in CA1 regions and gene deletion of EphA4 reduced the LTP in post-synaptic CA1 pyramidal cells (32).

SE and SRSs may damage neuron survival and stimulate tissue remodeling, including neurogenesis and astrogliosis. These processes require microvessels to supply abundant oxygen and nutrients to the damaged regions, which serves as a compensation mechanism. Epileptogenic brain injuries and seizures themselves may disturb blood-brain barrier permeability, increase the brain blood flow and trigger an increase in brain vascularity, which is associated with seizure frequency (33-35). Inhibition of tissue-type plasminogen activator and vascular endothelial growth factor (VEGF), or activation of erythropoietin and VEGFR2, are potential strategies for the treatment of epileptogenesis (36). In the present study, the vascular damage in the CA1 and CA3 areas began in the acute period following pilocarpine-induced SE. As a consequence, angiogenesis continued from the latency period to the chronic period in the areas where oxygen and glucose were required for tissue repair. Microvessel density increased compared to the control groups; these results are consistent with those of Rigau *et al* (35). However, Ndode-Ekane *et al* (10) demonstrated that the hippocampal vascular density decreases post-SE. These differences may be due to differences in animal species, immunopositive vascular markers and estimation methods. Notably, previous studies have suggested that the vascular plasticity in human TLE hippocampi is not true angiogenesis, and that the microvessels are actually atrophic, primarily with spine-like protrusions and a reduced lumen containing reactive astrocytes (37,38). As the objectives and methods were different from those in the present study, and the range of microvessel diameters is not defined, further studies are required to investigate the structural and functional features of the microvessels in the injured hippocampal regions during epileptogenesis.

In conclusion, the results of the present study demonstrated that angiogenesis occurs, and that the molecules EphA4 and ephrin-A5 are expressed in the hippocampal CA1 and CA3 areas throughout epileptogenesis. PECAM-1 may detect epileptic microvessel patterns in the hippocampi of mice and EphA4 may contribute to the microvessel plasticity via the ephrin-A5 signaling pathway. EphA4 may therefore be a potential target for clinical therapy.

Acknowledgements

The authors thank Miss. Jinghui Liang (Department of Neurology, Xiangya Hospital, Central South University, Changsha, China) for tissue preparation and Miss. Jinghui Liang, Dr Zhaohui Luo and Dr Zhiguo Wu (Department of Neurology, Xiangya Hospital, Central South University) for outstanding technical assistance. The present study was supported by the National Natural Science Foundation of China (grant nos. 81100967, 81371435 and 81401078) and the Specialized Research Fund for the Doctoral Program of Higher Education (grant no. 20110162120002).

References

1. Perry MS and Duchowny M: Surgical versus medical treatment for refractory epilepsy: Outcomes beyond seizure control. Epilepsia 54: 2060-2070, 2013.
2. Turski WA, Cavalheiro EA, Schwarz M, Czuczwar SJ, Kleinrok Z and Turski L: Limbic seizures produced by pilocarpine in rats: Behavioural, electroencephalographic and neuropathological study. Behav Brain Res 9: 315-335, 1983.
3. Curia G, Longo D, Biagini G, Jones RS and Avoli M: The pilocarpine model of temporal lobe epilepsy. J Neurosci Methods 172: 143-157, 2008.
4. Gröticke I, Hoffmann K and Löscher W: Behavioral alterations in the pilocarpine model of temporal lobe epilepsy in mice. Exp Neurol 207: 329-349, 2007.

5. Hu K, Li SY, Xiao B, Bi FF, Lu XQ and Wu XM: Protective effects of quercetin against status epilepticus induced hippocampal neuronal injury in rats: Involvement of X-linked inhibitor of apoptosis protein. Acta Neurol Belg 111: 205-212, 2011.
6. Zhang L, Hernández VS, Estrada FS and Luján R: Hippocampal CA field neurogenesis after pilocarpine insult: The hippocampal fissure as a neurogenic niche. J Chem Neuroanat 56: 45-57, 2014.
7. Noebels JL, Avoli M, Rogawski MA, Olsen RW, Delgado-Escueta AV, (eds): Jasper's Basic Mechanisms of the Epilepsies (Internet). 4th ed. Bethesda(MD): National Center for Biotechnology Information (US); 1-102, 2012.
8. Zha XM, Dailey ME and Green SH: Role of Ca^{2+}/calmodulin-dependent protein kinase II in dendritic spine remodeling during epileptiform activity in vitro. J Neurosci Res 87: 1969-1979, 2009.
9. Tang FR and Loke WK: Cyto-, axo- and dendro-architectonic changes of neurons in the limbic system in the mouse pilocarpine model of temporal lobe epilepsy. Epilepsy Res 89: 43-51, 2010.
10. Ndode-Ekane XE, Hayward N, Gröhn O and Pitkänen A: Vascular changes in epilepsy: Functional consequences and association with network plasticity in pilocarpine-induced experimental epilepsy. Neuroscience 166: 312-332, 2010.
11. Mosch B, Reissenweber B, Neuber C and Pietzsch J: Eph receptors and ephrin ligands: Important players in angiogenesis and tumor angiogenesis. J Oncol 2010: 135285, 2010.
12. Himanen JP, Rajashankar KR, Lackmann M, Cowan CA, Henkemeyer M and Nikolov DB: Crystal structure of an Eph receptor-ephrin complex. Nature 414: 933-938, 2001.
13. Smith FM, Vearing C, Lackmann M, Treutlein H, Himanen J, Chen K, Saul A, Nikolov D and Boyd AW: Dissecting the EphA3/Ephrin-A5 interactions using a novel functional mutagenesis screen. J Biol Chem 279: 9522-9531, 2004.
14. Greferath U, Canty AJ, Messenger J and Murphy M: Developmental expression of EphA4-tyrosine kinase receptor in the mouse brain and spinal cord. Mech Dev 119: (Suppl 1) S231-S238, 2002.
15. Jing X, Miwa H, Sawada T, Nakanishi I, Kondo T, Miyajima M and Sakaguchi K: Ephrin-A1-mediated dopaminergic neurogenesis and angiogenesis in a rat model of Parkinson's disease. PLoS One 7: e32019, 2012.
16. Omoto S, Ueno M, Mochio S and Yamashita T: Corticospinal tract fibers cross the ephrin-B3-negative part of the midline of the spinal cord after brain injury. Neurosci Res 69: 187-195, 2011.
17. Toyoda Y, Shinohara R, Thumkeo D, Kamijo H, Nishimaru H, Hioki H, Kaneko T, Ishizaki T, Furuyashiki T and Narumiya S: EphA4-dependent axon retraction and midline localization of Ephrin-B3 are disrupted in the spinal cord of mice lacking mDia1 and mDia3 in combination. Genes Cells 18: 873-885, 2013.
18. Khodosevich K, Watanabe Y and Monyer H: EphA4 preserves postnatal and adult neural stem cells in an undifferentiated state in vivo. J Cell Sci 124: 1268-1279, 2011.
19. Hara Y, Nomura T, Yoshizaki K, Frisén J and Osumi N: Impaired hippocampal neurogenesis and vascular formation in ephrin-A5-deficient mice. Stem Cells 28: 974-983, 2010.
20. Ogita H, Kunimoto S, Kamioka Y, Sawa H, Masuda M and Mochizuki N: EphA4-mediated Rho activation via Vsm-RhoGEF expressed specifically in vascular smooth muscle cells. Circ Res 93: 23-31, 2003.
21. Shu Y, Xiao B, Wu Q, Liu T, Du Y, Tang H, Chen S, Feng L, Long L and Li Y: The Ephrin-A5/EphA4 interaction modulates neurogenesis and angiogenesis by the p-Akt and p-ERK pathways in a mouse model of TLE. Mol Neurobiol 53: 561-576, 2016.
22. Gerlai R and McNamara A: Anesthesia induced retrograde amnesia is ameliorated by ephrinA5-IgG in mice: EphA receptor tyrosine kinases are involved in mammalian memory. Behav Brain Res 108: 133-143, 2000.
23. Goldshmit Y, Spanevello MD, Tajouri S, Li L, Rogers F, Pearse M, Galea M, Bartlett PF, Boyd AW and Turnley AM: EphA4 blockers promote axonal regeneration and functional recovery following spinal cord injury in mice. PLoS One 6: e24636, 2011.
24. Overman JJ, Clarkson AN, Wanner IB, Overman WT, Eckstein I, Maguire JL, Dinov ID, Toga AW and Carmichael ST: A role for ephrin-A5 in axonal sprouting, recovery, and activity-dependent plasticity after stroke. Proc Natl Acad Sci USA 109: E2230-E2239, 2012.
25. Ting MJ, Day BW, Spanevello MD and Boyd AW: Activation of ephrin A proteins influences hematopoietic stem cell adhesion and trafficking patterns. Exp Hematol 38: 1087-1098, 2010.
26. Li Y, Peng Z, Xiao B and Houser CR: Activation of ERK by spontaneous seizures in neural progenitors of the dentate gyrus in a mouse model of epilepsy. Exp Neurol 224: 133-145, 2010.
27. Goldshmit Y and Bourne J: Upregulation of EphA4 on astrocytes potentially mediates astrocytic gliosis after cortical lesion in the marmoset monkey. J Neurotrauma 27: 1321-1332, 2010.
28. Li J, Liu N, Wang Y, Wang R, Guo D and Zhang C: Inhibition of EphA4 signaling after ischemia-reperfusion reduces apoptosis of CA1 pyramidal neurons. Neurosci Lett 518: 92-95, 2012.
29. Murai KK, Nguyen LN, Irie F, Yamaguchi Y and Pasquale EB: Control of hippocampal dendritic spine morphology through ephrin-A3/EphA4 signaling. Nat Neurosci 6: 153-160, 2003.
30. Dudanova I, Kao TJ, Herrmann JE, Zheng B, Kania A and Klein R: Genetic evidence for a contribution of EphA:EphrinA reverse signaling to motor axon guidance. J Neurosci 32: 5209-5215, 2012.
31. Tremblay ME, Riad M, Bouvier D, Murai KK, Pasquale EB, Descarries L and Doucet G: Localization of EphA4 in axon terminals and dendritic spines of adult rat hippocampus. J Comp Neurol 501: 691-702, 2007.
32. Filosa A, Paixão S, Honsek SD, Carmona MA, Becker L, Feddersen B, Gaitanos L, Rudhard Y, Schoepfer R, Klopstock T, *et al*: Neuron-glia communication via EphA4/ephrin-A3 modulates LTP through glial glutamate transport. Nat Neurosci 12: 1285-1292, 2009.
33. Morin-Brureau M, Rigau V and Lerner-Natoli M: Why and how to target angiogenesis in focal epilepsies. Epilepsia 53: (Suppl 6) 64-68, 2012.
34. Romariz SA, Garcia Kde O, Paiva Dde S, Bittencourt S, Covolan L, Mello LE and Longo BM: Participation of bone marrow-derived cells in hippocampal vascularization after status epilepticus. Seizure 23: 386-389, 2014.
35. Rigau V, Morin M, Rousset MC, de Bock F, Lebrun A, Coubes P, Picot MC, Baldy-Moulinier M, Bockaert J, Crespel A and Lerner-Natoli M: Angiogenesis is associated with blood-brain barrier permeability in temporal lobe epilepsy. Brain 130: 1942-1956, 2007.
36. Kaminski RM, Rogawski MA and Klitgaard H: The potential of antiseizure drugs and agents that act on novel molecular targets as antiepileptogenic treatments. Neurotherapeutics 11: 385-400, 2014.
37. Kastanauskaite A, Alonso-Nanclares L, Blazquez-Llorca L, Pastor J, Sola RG and DeFelipe J: Alterations of the microvascular network in sclerotic hippocampi from patients with epilepsy. J Neuropathol Exp Neurol 68: 939-950, 2009.
38. Alonso-Nanclares L and Defelipe J: Alterations of the microvascular network in the sclerotic hippocampus of patients with temporal lobe epilepsy. Epilepsy Behav 38: 48-52, 2014.